AIAA JOURNAL
Vol. 31, No. 11, November 1993

Stability of a Fluid Surface in a Microgravity Environment

Jaume Casademunt,* Wenbin Zhang,† and Jorge Viñals‡
Florida State University, Tallahassee, Florida 32306
and
Robert F. Sekerka§
Carnegie Mellon University, Pittsburgh, Pennsylvania 15213

We introduce a stochastic model to analyze in quantitative detail the effect of the high-frequency components of the residual accelerations onboard spacecraft (often called *g* jitter) on the motion of a fluid surface. The residual acceleration field is modeled as a narrow-band noise characterized by three independent parameters: its intensity G^2, a dominant frequency Ω, and a characteristic spectral width τ^{-1}. The white noise limit corresponds to $\Omega\tau \to 0$, with $G^2\tau$ finite, and the limit of a periodic *g* jitter (or deterministic limit) can be recovered for $\Omega\tau \to \infty$, G^2 finite. Analysis of the linear response of a fluid surface subjected to a fluctuating gravitational field leads to the stochastic Mathieu equation driven by both additive and multiplicative noise. We discuss the stability of the solutions of this linear equation in the two limits of white noise and deterministic forcing, and in the general case of narrow-band noise. The results are then applied to typical microgravity conditions.

Introduction

A STOCHASTIC model is introduced to describe the high-frequency components of the residual accelerations onboard spacecraft (often called *g* jitter). The model is incorporated into the equations governing fluid motion, and the stability of a surface of discontinuity between two fluids of different density is analyzed. The linear stability of this surface is governed by the stochastic Mathieu equation, driven by both multiplicative and additive noise. We study the range of parameters in which the solutions of the stochastic Mathieu equation are stable and apply the results to a water-air surface in typical microgravity conditions. We find that the component of *g* jitter normal to the surface at rest couples nonlinearly to the surface displacement and can lead to parametric instability. On the other hand, the two parallel components appear additively, and we show that they do not modify the linear stability boundaries associated with the normal component.

A certain amount of attention has been paid recently to modeling *g* jitter as a periodic function of time,[1-3] but little attention has been paid to the more realistic case in which the effective acceleration spectrum contains a band of frequency components and is random in nature. Early work in this direction by Antar[4] considered the stability of the Rayleigh-Bénard configuration under a random gravitational field with a uniform frequency spectrum (white noise). Later, Fichtl and Holland[5] used a stochastic description to study the distribution of impulses that would exceed a prescribed threshold.

We introduce a general model for *g* jitter, also based on a stochastic description,[6] with a spectrum that is similar to residual acceleration spectra measured in space missions. The model, which we call narrow-band noise, is characterized by three parameters: the mean intensity of the fluctuations G^2; their characteristic angular frequency Ω; and the characteristic width of the spectrum (peaked at Ω) τ^{-1} (Ref. 7). In the limit $\Omega\tau \to 0$, with $D = G^2\tau$ finite, narrow-band noise reduces to white noise of intensity D, whereas for $\Omega\tau \to \infty$ and G^2 finite, monochromatic noise of intensity G^2 is recovered. Individual realizations of monochromatic noise are sinusoidal functions with frequency Ω but with random amplitudes and phases. From published acceleration spectra measured during space missions,[2,3] one can infer that characteristic frequencies of *g* jitter are in the range 1–20 Hz, hence $\Omega \sim 2\pi$ (1–20) s^{-1}. Characteristic widths of the spectral density are 5–10 Hz, or $\tau \sim 0.1$–0.2 s. Therefore, $\Omega\tau \sim 1$–25, which is an intermediate case between the white noise limit and the deterministic limit of periodic forcing.

The motivation for our work is that high-frequency components of the residual acceleration field will affect fluid flow primarily in regions where large gradients of density exist. The case of a surface of discontinuity studied in this paper is a prototypical example and is used to explore in detail the coupling between a time-dependent acceleration and fluid motion due to density gradients. Because our analysis leads to the stochastic Mathieu equation, our results are applicable to a variety of situations, including parametrically excited surface waves[8] and convective instabilities in systems under a time-dependent gravitational field.[9]

Our results show that linear instability in the stochastic case is mainly due to subharmonic parametric resonance. There is, however, a complex interplay between the linear dispersion relation of the surface and the power spectrum of the external acceleration field that results in two main differences with respect to the classical deterministic case of periodic forcing. First, stochastic forcing excites a range of frequencies. Parametric resonance can occur for modes which would not be resonant with the exciting frequency in a deterministic model. Second, stability is typically enhanced when the spectral width of a stochastic forcing is increased.

Equation Governing Interface Displacements

Consider two incompressible, immiscible fluids in a finite container, initially separated by a planar surface at $z = 0$. We assume that fluid 1 of density ρ_1 and shear viscosity μ_1 occupies the region $-d < z < 0$, and fluid 2 of density ρ_2 and shear viscosity μ_2 occupies the region $0 < z < d$. We summarize here the conditions under which the fluid equations can be reduced to a closed equation for the interface displacement alone when the system is subjected to arbitrary, time-dependent accelerations $\boldsymbol{g}(t) = [g_x(t), g_y(t), g_z(t) - g_0]$. Here, g_0 is a static component of the acceleration directed along the z axis. As discussed in Ref. 7, an equation for the interface displacement alone only exists when the time scales associated with viscous dissipation are much longer than typical time scales of interface motion (i.e., in the underdamped limit). In this regime, fluid flow can be assumed to be potential except in thin boundary layers near the container walls and the fluid interface.

Received Nov. 1, 1992; presented as Paper 93-0911 at the AIAA 31st Aerospace Sciences Meeting, Reno, NV, Jan. 11–14, 1993; revision received March 25, 1993; accepted for publication March 26, 1993.

*Postdoctoral Associate, Supercomputer Computations Research Institute.
†Graduate Student, Supercomputer Computations Research Institute.
‡Research Scientist, Supercomputer Computations Research Institute.
§Professor, Department of Physics and Mathematics.

We will neglect in what follows any capillary effects at the contact between the interface and the container wall.

Following the formulation of Miles,[10] we expand both the interface displacement $h(x,y,t)$ away from its reference position and the velocity potential $\phi_i(x,y,z,t)$ ($i = 1,2$ denotes the two fluids) as

$$h(x,y,t) = \sum_n h_n(t)\,\psi_n(x,y) \tag{1}$$

$$\phi_i(x,y,z,t) = \sum_n \phi_{in}(t)\,\psi_n(x,y)\,Z_{in}(z) \tag{2}$$

where $\psi_n(x,y)$ are the eigenfunctions of $(\nabla^2 + k_n^2)\psi_n(x,y) = 0$ with boundary condition $\hat{n}\cdot\nabla\psi_n = 0$ at the container's wall. The equation for ψ_n follows from Laplace's equation for the velocity potentials ϕ_i, when their z dependences are solved for each eigenmode as $Z_{1n} = \cosh k_n(z + d)/\cosh k_n d$ and $Z_{2n} = \cosh k_n(z - d)/\cosh k_n d$. Here, d is the depth of the fluid layer, which is assumed to be equal in both fluids for simplicity. The eigenfunctions are orthogonal and normalized, $\int\int \psi_m\psi_n\,dx\,dy = S\delta_{mn}$, with S the cross-sectional area of the container. If cubic and higher orders terms in h_n and $\dot{h}_n$ are neglected, the Lagrangian function for the generalized coordinates $h_n(t)$ reads

$$L = \sum_n (\rho_1+\rho_2) S \left(\frac{\dot{h}_n^2}{2k_n'} - \frac{1}{2} A\,[g_0 - g_z(t)]\,h_n^2 + A Q_n(t)\,h_n - \frac{\Gamma k_n^2 h_n^2}{2(\rho_1+\rho_2)} \right) \tag{3}$$

where $k_n' = k_n \tanh(k_n d)$, $A = (\rho_1-\rho_2)/(\rho_1+\rho_2)$, Γ is the interfacial tension, and

$$Q_n(t) = \frac{1}{S}\int\int [g_x(t)x + g_y(t)y]\psi_n\,dx\,dy \tag{4}$$

Weak viscous dissipation may now be approximately incorporated by calculating the rate of energy dissipation $\mathcal{D}$ of the fluid system. By introducing the dissipation function $\mathcal{F} = -\mathcal{D}/2$, we have the following equation governing the motion of the viscous fluid,

$$\frac{d}{dt}\left(\frac{\partial L}{\partial \dot{h}_n}\right) - \frac{\partial L}{\partial h_n} + \frac{\partial \mathcal{F}}{\partial \dot{h}_n} = 0 \tag{5}$$

As discussed in the Appendix, for a large enough container the dissipation function $\mathcal{F}$ can be approximately written as

$$\mathcal{F} \approx \frac{1}{2} S(\rho_1+\rho_2)\sum_n \frac{\gamma_n}{k_n'}\dot{h}_n^2 \tag{6}$$

then Eq. (5) reads

$$\frac{d^2 h_n}{dt^2} + \gamma_n \frac{dh_n}{dt} + [\omega_n^2 - A k_n' g_z(t)]\,h_n = A k_n' Q_n(t) \tag{7}$$

with

$$\omega_n^2 = \frac{(\rho_1-\rho_2)g_0 k_n' + \Gamma k_n^2 k_n'}{\rho_1+\rho_2} \tag{8}$$

The damping coefficient γ_n contains a contribution from bulk dissipation $4[(\mu_1+\mu_2)/(\rho_1+\rho_2)]k_n^2$, and a contribution from dissipation at the interface boundary layer which is, in a order of magnitude estimation, proportional to $\sqrt{\nu}$, with ν the average kinematic viscosity of the two fluids. For the special case of a single fluid, the dissipation in the free surface boundary layer can be neglected in the underdamped limit.[7] Viscous dissipation in the boundary layer near the container wall cannot be written in the form of Eq. (6). In this paper we consider only a large enough container such that dissipation near container's wall is small compared to other sources of dissipation. See the Appendix for a quantitative estimation.

Equation (7) is our starting point for the stochastic analysis presented in the next section. The salient feature of Eq. (7) is that the contribution of $g_z(t)$ is nonlinear or multiplicative $[g_z(t)h_n(t)]$, whereas the contributions from $g_x(t)$ and $g_y(t)$ are additive. It can also be shown that, contrary to the multiplicative forcing, the strength of the additive forcing is size dependent and vanishes in the limit of an infinite cross-sectional area. For instance, in a rectangular container $L_x \times L_y$, Eq. (4) with the explicit form of the corresponding eigenfunctions can be written as

$$Q_{ij}(t) = \frac{\sqrt{2}}{k_{ij}^2}\left(\frac{[(-1)^i - 1]\,g_x(t)}{L_x}\delta_{j0} + \frac{[(-1)^j - 1]\,g_y(t)}{L_y}\delta_{i0} \right) \tag{9}$$

In the limit of an infinite container $L_x, L_y \to \infty$, $Q_{ij}(t) \to 0$ for any fixed wave number k_{ij}. Recall that we consider a large container to neglect the viscous dissipation near the container wall. Therefore, the analysis on the effect of additive forcing Q_n to the stability of a fluid interface is relevant for the case of a large but finite container.

Oscillator Driven by Multiplicative and Additive Noise

We have seen that under certain conditions, each normal mode of the interface displacement satisfies a closed equation that is equivalent to that of a linear oscillator subject to both multiplicative and additive forcing. The intensity of the additive forcing depends on system size but not on the actual interface displacement and vanishes in the limit of an infinite system size. The intensity of the multiplicative term is independent of system size but depends on the actual displacement of the interface and vanishes in the reference state of a planar interface at $z = 0$.

We rewrite Eq. (7) as

$$\frac{d^2 x}{dt^2} + \gamma\frac{dx}{dt} + \omega_0^2 x + \xi(t)\,x = \zeta(t) \tag{10}$$

where $x(t)$ corresponds to any of the eigenmodes h_n and $\xi(t)$ and $\zeta(t)$ are two stochastic forces. In this section we study the statistical properties of the dynamical variable $x(t)$. We characterize the stability of the solutions in terms of the stability of the statistical moments of $x(t)$ as a function of the parameters of the system (γ and ω_0) and of the noise. We restrict our study here to the second-order moments, $\langle x^2\rangle$, $\langle x\dot{x}\rangle$, and $\langle \dot{x}^2\rangle$, that are directly proportional to the energy of the oscillations.

Uncorrelated White Noises

If the two stochastic forces in Eq. (10) are white and uncorrelated, $\langle \xi(t)\,\xi(t')\rangle = 2D\delta(t-t')$, $\langle \zeta(t)\,\zeta(t')\rangle = 2\varepsilon\delta(t-t')$, and $\langle \xi(t)\,\zeta(t')\rangle = 0$, the evolution equation for the second-order moments is closed and linear. The so-called energetic instability occurs when one of the three eigenvalues of the evolution matrix for the second-order moments, say λ_1, has a positive real part, implying an exponential growth of the second moments. This eigenvalue is known exactly[11] and in the underdamped limit $\gamma^2/4\omega_0^2 \ll 1$ reads

$$\lambda_1 = -\gamma + D/\omega_0^2 \tag{11}$$

and is independent of the intensity of the additive noise ε. The white noise limit corresponds to the idealized situation in which the spectrum of the stochastic force is constant. For more realistic noise spectra, the evolution equations for the second-order moments are not closed in general, and to define a similar criterion of instability, different truncation schemes have to be invoked.

Deterministic Periodic Forcing

The opposite limit to white noise corresponds to a periodic forcing of the form $\xi(t) = \xi_0 \cos \Omega t$ and $\zeta(t) = \zeta_0 \cos(\Omega t + \phi_0)$. This limit models a monochromatic g jitter of frequency Ω with highly correlated components. In this limit, the stability properties of Eq. (10) can be determined as follows. In the absence of the additive term ($\zeta_0 = 0$), Eq. (10) reduces to the classical (damped) Mathieu equation. For $\gamma = 0$, the solutions are always stable and periodic for small enough ξ_0, except at the so-called parametric resonances that occur when $\omega_0 = n\Omega/2$, with $n = 1, 2, \ldots$. The strongest resonance occurs at $n = 1$. For finite γ, however, there is a finite threshold for instability

$$(\xi_0/2\omega_0)^2 - \gamma^2 \geq 0 \tag{12}$$

We argue that the regions of stability of the solutions of the damped Mathieu equation do not depend on an additive periodic forcing of the same period. This result follows from general theorems of linear differential equations with periodic coefficients. According to Sec. 2.9 in Ref. 12, if the homogeneous part of Eq. (10) does not have periodic solutions, and the inhomogeneous term is itself periodic with the same period as the coefficients of the homogeneous part, then the particular solution of the full equation is itself a periodic function. Therefore, the stability of the solutions of the full equation remains unchanged after the addition of the inhomogeneous terms, since instability will only occur if the homogeneous part already has a positive Floquet exponent. In our case, the Floquet exponents of the homogeneous part α_1, α_2 (i.e., of the damped Mathieu equation) are related to those of the undamped case $\pm\sigma$ by $\alpha_{1,2} = -\gamma/2 \pm \sigma$ (see Sec. 4.3 in Ref. 12). Therefore, the solutions of the homogeneous equation are not periodic except when $\gamma = 2\sigma$. But this is precisely the condition defining the stability boundary of the damped Mathieu equation. Therefore, the stability boundaries of Eq. (10) for the deterministic case are also insensitive to additive forcing.

Narrow-Band Noise

We now consider the generic case of a narrow-band noise. We have shown that the additive contribution to Eq. (10) does not modify the stability boundaries of the second-order moments in the two limits of white noise and deterministic forcing. It is natural to expect that in the intermediate case of narrow-band noise, which interpolates between the two limits, the presence of an additive noise, even if highly correlated to the multiplicative noise, will not affect the stability boundaries either. Therefore, we restrict our stability study for narrow-band noise to the multiplicative contribution in Eq. (10). We define the spectrum of narrow-band noise as

$$P_\xi(\omega) = \frac{1}{2\pi}\langle\xi^2\rangle\tau\left(\frac{1}{1+\tau^2(\Omega+\omega)^2} + \frac{1}{1+\tau^2(\Omega-\omega)^2}\right) \tag{13}$$

This spectrum corresponds to a correlation function of the form

$$\langle\xi(t)\,\xi(t')\rangle = \langle\xi^2\rangle e^{-|t-t'|/\tau}\cos\Omega(t-t') \tag{14}$$

The limit $\Omega\tau \to 0$, $\langle\xi^2\rangle\tau = D$ finite, corresponds to white noise of intensity D. In the opposite limit, monochromatic noise or, equivalently, a periodic forcing of amplitude ξ_0 is recovered with $\langle\xi^2\rangle = \xi_0^2/2$.

We have investigated this case by perturbation theory and by numerical means.[7] We have shown that the underlying mechanism of instability in the stochastic case can also be understood as a parametric instability. For a wide range of parameters of the noise, it is shown in Ref. 7 that the eigenvalue describing the stability of the second moments is well approximated by the expression

$$\lambda_1 \simeq -\gamma + (1/\omega_0^2)\,\pi P_\xi(2\omega_0) \tag{15}$$

The dependence of the instability threshold on the value of the power spectrum at precisely $2\omega_0$ reflects the fact that the underlying mechanism for instability can still be understood as subharmonic parametric resonance.

Effect of Additive Noise

Additive noise in Eq. (10) simply modifies the spectrum of excitations of the interface in the cases in which the interface is stable. For $\lambda_1 > 0$ the average energy of the oscillations diverges exponentially in time, until nonlinearities saturate the growth. The presence of additive noise is irrelevant. On the other hand, for $\lambda_1 < 0$ additive noise determines a finite steady value for the second moments, which would vanish if only multiplicative noise were present.

To discuss the influence of the additive term on the steady-state fluctuations of the interface, let us first consider Eq. (10) without multiplicative noise [$\xi(t) = 0$]. Equation (10) becomes linear, and the effect of a noise comprising a band of frequency components can be described as a linear superposition of the solution of the oscillator forced by a single frequency component. The power spectrum $P(\omega)$ of the process $x(t)$ is defined in the stationary regime as[13]

$$P(\omega) = \frac{1}{2\pi}\int_{-\infty}^{\infty} e^{-i\omega s}\langle x(t)\,x(t+s)\rangle\,\mathrm{d}s \tag{16}$$

Equation (10) with $\xi(t) = 0$ reads, in Fourier space,

$$-\omega^2\hat{x}(\omega) + i\omega\gamma\hat{x}(\omega) + \omega_0^2\hat{x}(\omega) = \hat{\zeta}(\omega) \tag{17}$$

By using Eq. (17) and the relations (Ref. 13) $\langle\hat{x}(\omega)\,\hat{x}^*(\omega')\rangle = \delta(\omega-\omega')P(\omega)$ and $\langle\hat{\zeta}(\omega)\,\hat{\zeta}^*(\omega')\rangle = \delta(\omega-\omega')P_\zeta(\omega)$, we have

$$P(\omega) = \frac{P_\zeta(\omega)}{[\omega_0^2-\omega^2]^2+\gamma^2\omega^2} \tag{18}$$

where $P_\zeta(\omega)$ is the power spectrum of the additive noise. Finally, by using Eq. (16) the second moment $\langle x^2\rangle$ can be written as $\langle x^2\rangle = \int_{-\infty}^{\infty} P(\omega)\,\mathrm{d}\omega$. In the deterministic limit, we have $P_\zeta(\omega) = 1/2\zeta_0\,\delta(\omega-\Omega)$ and

$$\langle x^2\rangle = \frac{1}{2}\frac{\zeta_0}{[\omega_0^2-\Omega^2]^2+\gamma^2\Omega^2} \tag{19}$$

where the average is now understood over a period in the stationary regime. For white noise, we have $P_\zeta(\omega) = \varepsilon/\pi$ and

$$\langle x^2\rangle = \varepsilon/(2\gamma\omega_0^2) \tag{20}$$

For narrow-band noise, the second moment can be expressed as

$$\langle x^2\rangle = \frac{\langle\zeta^2\rangle\tau}{2\pi}\int_{-\infty}^{\infty}\frac{\mathrm{d}\omega}{[\omega_0^2-\omega^2]^2+\gamma^2\omega^2} \times\left(\frac{1}{1+\tau^2(\Omega+\omega)^2}+\frac{1}{1+\tau^2(\Omega-\omega)^2}\right) \tag{21}$$

The excitation mechanism in all of these cases is an ordinary resonance phenomenon in contrast with the parametric resonance of the multiplicative case. In both the multiplicative and additive cases, the variable x responds in time with the characteristic frequency of the forcing Ω, but in the purely additive case the oscillations have a finite amplitude that depends on Ω and the characteristic frequency of the oscillator ω_0. Unlike the multiplicative case, the amplitude of oscillation saturates due to the dissipative forces even within the linear regime, and instability in the sense of exponential growth of the second moments cannot occur.

Higher Order Moments

In the general case in which both noise contributions are present but the system is below threshold for parametric instability, the distribution of fluctuations of the interface displacement cannot be determined exactly for narrow-band noise. In the limit in which both noises are white, it has been shown in Ref. 11 that the distribution $P(E)$ of the energy of the oscillations $E = 1/2(\dot{x}^2 + \omega_0^2 x^2)$ (in the envelope approximation, which assumes that the time scale for change of E is much larger than that of $x,\dot{x}$) is given by

$$P(E) = \frac{\gamma\omega_0^2 - D}{2\omega_0^2\varepsilon}\left(\frac{1}{[1 + (D/2\varepsilon\omega_0^2)E]^{\gamma\omega_0^2/D}}\right) \tag{22}$$

In the limit $D \to 0$ (purely additive driving), Eq. (22) is replaced by

$$P(E) = \frac{\gamma}{\varepsilon}\exp(-\gamma E/\varepsilon) \tag{23}$$

Equations (22) and (23) clearly illustrate how the probability distribution of amplitude fluctuations is qualitatively modified by the presence of multiplicative noise. The dependence of $P(E)$ on E is a power law in the multiplicative case as opposed to the exponential decay for the additive case. As a consequence, moments of $P(E)$ for the multiplicative case diverge beyond an order that depends on D, γ, and ω_0, but not on the additive noise intensity ε. Hence, in the white noise limit, there are always moments of sufficiently high order that are unstable. For narrow-band noise, the stability boundaries of the various moments are also expected to depend on the order of the moments considered. However, the stability boundaries for all of the various moments have to converge to the stability diagram of the deterministic case, as one narrows the width of the noise spectrum.

In summary, the stability of the solutions of Eq. (10) is determined solely by the multiplicative noise. Above threshold, the second-order moments grow exponentially in time and additive noise is irrelevant. If all of the interface modes are below threshold, which modes are predominantly excited is determined by the dominant frequencies of the additive noise. Higher order moments of the interface displacement, however, may depend strongly on the parameters of the multiplicative noise.

Application to Typical Microgravity Conditions

Although a precise characterization of residual accelerations in a microgravity environment is under way, there is enough information already available for our purposes. The spectral density of g jitter determined during various space missions does have one or several dominant frequencies, but it is also quite broad.

Contact with the results obtained for the stochastic oscillator can be made in the case of a single fluid in an infinite container by replacing $\gamma = 4\nu q^2$, $\omega_0^2 \approx (\Gamma/\rho)q^3$, and $\xi(t) = qg_z(t)$, where q is the wave number of the surface displacement away from planarity. Now $\langle\xi^2\rangle = q^2\langle g_z^2\rangle$, with $\langle g_z^2\rangle$ being proportional to the area beneath the spectral density of g jitter measured. From Fig. 9 in Ref. 3 (which gives the power spectral density of a representative time window aboard Spacelab 3), we estimate $G = \sqrt{\langle g_z^2\rangle} \approx 8 \times 10^{-4} g_E$. This is a very conservative estimate; considerably larger values can be obtained from this and other published measurements (see, e.g., Figs. 1 and 2 in Ref. 2). Note also that both γ and ω_0 depend on the wave number q, as a result of this in the limit $\omega_0 \to 0$ the system is actually approaching the underdamped limit, $\gamma^2/4\omega_0^2 = 4\nu^2\rho\Gamma^{-1}q \ll 1$. The stability boundary given by Eq. (15) can be explicitly written for this case as

$$\frac{G_c^2}{\nu\Omega^3} = 4\frac{\omega_0^2}{\Omega^2}\left(\frac{1 + 2(\Omega\tau)^2[1 + 4(\omega_0/\Omega)^2]}{\Omega\tau\{1 + (\Omega\tau)^2[1 + 4(\omega_0/\Omega)^2]\}}\right.$$
$$\left. + \frac{(\Omega\tau)^4[1 - 4(\omega_0/\Omega)^2]^2}{\Omega\tau\{1 + (\Omega\tau)^2[1 + 4(\omega_0/\Omega)^2]\}}\right) \tag{24}$$

where G_c is the critical value for instability. Equation (24) is plotted in Fig. 1 for several representative values of $\Omega\tau$. The regions above the curves correspond to regions of instability. The figure also shows that there is a critical value of $\Omega\tau$ at which the curves change from monotonic to nonmonotonic behavior. The critical value is $(\Omega\tau)_c \simeq 1.555$. The minimum at $\omega_0/\Omega = 0$ is a zero of the function and is independent of $\Omega\tau$. The second minimum corresponds to the modes that resonate with the dominant frequen-cies of the spectrum. For increasing $\Omega\tau$ this minimum approaches $\omega_0 = \Omega/2$ from the left. The corresponding value of $G_c^2/\nu\Omega^3$ decreases, as the spectrum becomes narrower around Ω favoring the resonance.

For a given spectrum of g jitter, there is always a band of unstable modes at low frequencies (long wavelengths). As we increase $\Omega\tau$ this band becomes narrower, and the critical wavelength for this low-frequency instability increases. For $\Omega\tau > (\Omega\tau)_c$ a second band of unstable modes approximately centered at $\omega_0/\Omega = 0.5$ may appear depending on the level of g jitter. For the parameter ranges estimated for typical g jitter, the low-frequency instability is likely to be unobservable because it may correspond to wavelengths larger than the natural long wavelength cutoff defined by the container size. For instance, for fluid parameters appropriate to a water-air interface, $\nu = 0.01$ cm^2/s, $\Gamma = 75.5$ erg/cm^2, and $\rho = 1$g/cm^3; with $\Omega/2\pi \sim 12$ Hz and $G \sim 10^{-3} g_E$ the critical wavelength ranges from ~ 15 cm to ~ 35 cm for $\Omega\tau$ in the range from 1 to 25.

Given that the low-frequency band is likely not to be observable, the absolute threshold for instability will typically be given by the minimum of the curve from Eq. (24). In Fig. 2 we have plotted the threshold given by Eq. (24) at $\omega = \Omega/2$, as a function of Ω for several values of τ [the minimum of Eq. (24) is not exactly at $\omega = \Omega/2$, but the value of $G^2/\nu\Omega^3$ at the exact minimum and at $\omega = \Omega/2$ do not differ significantly]. The dashed portion of the curve corresponds to the region where there is no resonance minimum [$\Omega\tau < (\Omega\tau)_c$]. For comparison purposes, we have also plotted the deterministic case given by $\xi(t) = \xi_0 \cos \Omega t$ [the threshold for instability because of subharmonic resonance in this case is given in Eq. (12)]. To compare this case with the stochastic case, we have $\langle\xi^2\rangle = \xi_0^2/2$, i.e., $q^2\langle g_z^2\rangle = \xi_0^2/2$. The threshold for instability of the resonant mode with $\omega_0 = \Omega/2$ in this case is given by

$$(G_c)_{\text{det}} = \nu\sqrt{2}\left(\frac{2\rho\Omega^5}{\Gamma}\right)^{1/3} \tag{25}$$

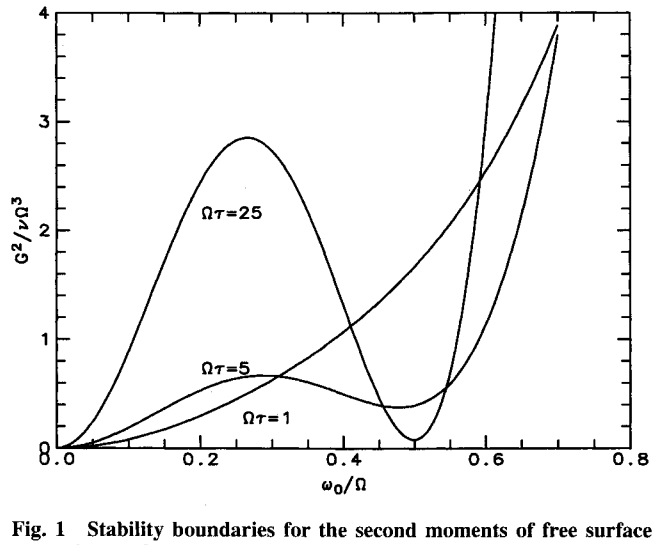

Fig. 1 Stability boundaries for the second moments of free surface away from planarity. The figure shows the dimensionless mean squared fluctuations in gravitational acceleration vs the dimensionless frequency of the surface modes. The intensity of the fluctuations in the gravitational field is given by $G^2 = \langle g_z(t)^2\rangle$. Different curves show the stability boundaries for various values of the dimensionless correlation time $\Omega\tau$. We note that for $\Omega\tau \geq 1.555$, the neutral stability curve has one minimum at a finite value of ω_0/Ω. Below that value, the only minimum is at $\omega_0/\Omega = 0$.

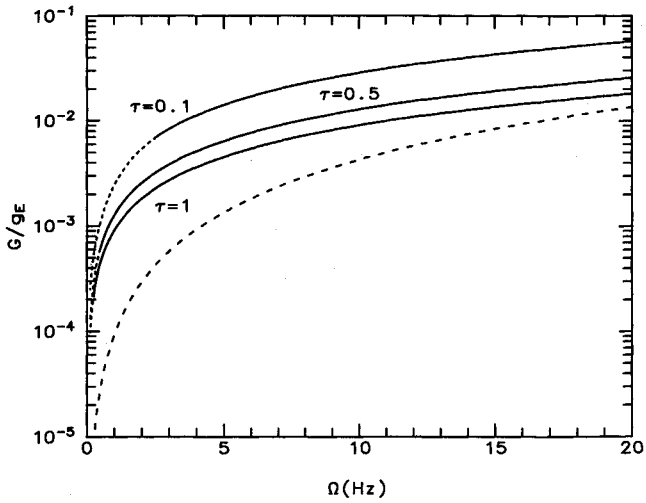

Fig. 2 Estimate of tolerable levels of g jitter for instability of a planar water-air surface at room temperature. We show the normalized root mean squared g jitter for instability as a function of the characteristic frequency of the driving noise (g_E is the intensity of the gravitational field on the Earth's surface). Three different correlation times are shown. The solid lines refer to those regions of $\Omega\tau$ for which the stability curve has a minimum at finite frequencies (see Fig. 1). The dotted lines represent the stability boundary at $\omega_0 = \Omega/2$, even though the stability curve does not have a minimum at this point. The dashed line is the stability curve for the damped Mathieu equation for the same driving frequency.

For the range of frequencies 5–20 Hz, we see that a g jitter level of $G \simeq 10^{-3} g_E$ lies below all of the curves, and therefore it does not lead to instability.

Finally, Fig. 1 also shows that the interface becomes effectively more stable as τ is decreased, at constant G (i.e., at constant area of the power spectrum). The forcing is less efficient in exciting the resonance as it spreads into a wider band of frequencies, as opposed to being concentrated at the resonant frequency.

Appendix: Estimation of Various Contributions to Viscous Dissipation

Here we discuss in some detail the estimation of the different contributions to the total dissipation rate.

Viscous dissipation in the fluid system can be split into three different contributions, namely, dissipation in the bulk, in the interface boundary layer, and in the boundary layer near the container's wall. Dissipation due to potential flow in the bulk can be written as[14]

$$\mathcal{D}_{\text{bulk}} = -2\mathcal{F}_{\text{bulk}} = -2\mu_1 \int_{V_1} \left(\frac{\partial^2 \phi_1}{\partial x_i \partial x_j} \right)^2 dV - 2\mu_2 \int_{V_2} \left(\frac{\partial^2 \phi_2}{\partial x_i \partial x_j} \right)^2 dV \tag{A1}$$

where the integrals extend over the volume occupied by fluids 1 and 2, respectively. When the nonlinear contributions in the interfacial displacement are neglected, we find

$$\mathcal{F}_{\text{bulk}} = (\mu_1 + \mu_2) \left[2S \sum_n \frac{k_n^2}{k_n'} \dot{h}_n^2(t) + \sum_{mn} \frac{\dot{h}_m \dot{h}_n}{k_m' k_n'} P_{mn} \int_{-d}^{0} dz\, Z_{1m}(z) Z_{1n}(z) \right] \tag{A2}$$

where $P_{mn} = \int\int dx\, dy\, \nabla^2(\nabla\psi_m \cdot \nabla\psi_n)$. The matrix P_{mn} depends on the geometry of the container and, in general, is neither zero nor diagonal. Therefore, the equation for $h_n(t)$ is coupled in general to all of the other modes $h_m(t)$. In the case of a rectangular container of sides L_x and L_y, the eigenfunctions ψ_n are

$$\psi_{i,j}(x,y) = \sqrt{(2-\delta_{i0})\,(2-\delta_{j0})} \cos\frac{i\pi x}{L_x} \cos\frac{j\pi y}{L_y} \tag{A3}$$

where $i,j = 0,1,2,\ldots$, except $i=j=0$, and we have $P_{mn} = 0$ for all m,n. For arbitrary geometry, P_{mn} is expected to vanish in the limit of large system size.

Dissipation in the viscous boundary layer near the container's wall can be estimated by assuming a constant gradient of velocity in the boundary layer for each eigenmode. The thickness of the boundary layer for mode n is $\delta_n = \sqrt{2\nu/\omega_n}$, with ω_n the characteristic angular frequency of nth mode. Then,

$$\mathcal{D}_{\text{wall}} \sim -\left(\rho_1 \sqrt{\nu_1/2} + \rho_2 \sqrt{\nu_2/2} \right) \sum_{mn} \frac{\sqrt{\omega_m} + \sqrt{\omega_n}}{2 k_m' k_n'} f_{mn} \dot{h}_m \dot{h}_n \tag{A4}$$

where

$$f_{mn} = \int_{S_{1w}} dS \nabla[\psi_m Z_{1m}(z)] \cdot \nabla[\psi_n Z_{1n}(z)] = \int_{S_{2w}} dS \nabla[\psi_m Z_{2m}(z)] \cdot \nabla[\psi_n Z_{2n}(z)]$$

S_{1w} and S_{2w} are the surfaces of the container wall in contact with fluids 1 and 2, respectively. The matrix f_{mn} is not diagonal in general and can be estimated to be of order $\sim 2L k_m k_n/(k_m + k_n)$ with L the lateral size of the container. With this estimation the ratio of bulk dissipation to the dissipation near the container's wall is of the order of $\sim L k_n^2 \sqrt{2\nu/\omega_n}$. Therefore, for a given driving frequency range and the concomitant resonant modes k_n, the dissipation near the container's wall is not important provided the system size is large enough. For a water-air interface and a typical g jitter frequency of ~ 10 Hz, bulk dissipation dominates for $L > 5$ cm.

We now estimate dissipation in the boundary layer at the fluid interface between two fluids. Again, we assume a constant gradient of velocity inside the boundary layer for each eigenmode and equal to $|\phi_{1n}(t)\nabla(\psi_n Z_{1n}) - \phi_{2n}(t)\nabla(\psi_n Z_{2n})|/\delta_n$, with $\delta_n = \sqrt{2\nu/\omega_n}$. Here ν and μ are the average kinematic and dynamic viscosities of the two fluids. Then we find

$$\mathcal{D}_{\text{int}} \sim -4S\mu \sum_n \sqrt{\frac{\omega_n}{2\nu}} \frac{k_n^2}{k_n'^2} \dot{h}_n^2 \tag{A5}$$

This contribution dominates over bulk dissipation, even in the underdamped limit and for a large container. The frequency dependence of the resulting damping coefficient implies that a closed equation for $h_n(t)$ cannot be obtained in the general case of a time-dependent gravitational field. If, on the other hand, the gravitational field is constant, Eq. (7) is approximately valid and contains a damping coefficient that depends on the frequency of the mode considered. Finally, in the case of the free surface of a fluid ($\rho_2 = 0$, $\mu_2 = 0$), the dissipation in the free surface boundary layer can be neglected in the underdamped limit, as discussed in Ref. 7.

Acknowledgments

This work is supported by the Microgravity Science and Applications Division of NASA under Contract NAG3-1284. This work is also supported in part by the Supercomputer Computations Research Institute, which is partially funded by the U.S. Department of Energy, Contract DE-FC05-85ER25000. We thank Vlad Shapiro for many interesting discussions.

References

[1]Walter, H. U. (ed.), *Fluid Sciences and Materials Sciences in Space*, Springer-Verlag, New York, 1987, Chaps. 1, 18.

[2]Alexander, J. I. D., "Low-Gravity Experiment Sensitivity to Residual Acceleration: A Review," *Microgravity Science and Technology,* Vol. 3, No. 2, 1990, pp. 52–67.

[3]Nelson, E. S., "An Examination of Anticipated g-Jitter on Space Station and Its Effects on Materials Processes," NASA TM 103775, May 1991.

[4]Antar, B. N., "Thermal Instability of Stochastically Modulated Flows," *Physics of Fluids,* Vol. 20, No. 10, 1977, pp. 1785–1787.

[5]Fichtl, G. H., and Holland, R. L., "Simplified Model of Statistically Stationary Spacecraft Rotation and Associated Induced Gravity Environments," NASA TM 78164, Feb. 1978.

[6]Viñals, J., and Sekerka, R. F., "Effect of g-jitter on the Spectrum of Excitations of a Free Fluid Surface: Stochastic Formulation," AIAA Paper 90-0652, Jan. 1990.

[7]Zhang, W., Casademunt, J., and Viñals, J., "Study of the Parametric Oscillator Driven by Narrow Band Noise to Model the Response of a Fluid Surface to Time-Dependent Accelerations," *Physics of Fluids A* (to be published, 1993).

[8]Miles J., and Henderson, D., "Parametrically Forced Surface Waves," *Annual Review of Fluid Mechanics,* Vol. 22, Annual Review, Palo Alto, CA, 1990, pp. 143–165.

[9]Wheeler, A. A., McFadden, G. B., Murray, B. T., and Coriell, S. R., "Convective Stability in the Rayleigh-Bénard and Directional Solidification Problems: High Frequency Gravity Modulation," *Physics of Fluids A,* Vol. 3, No. 3, 1991, pp. 2847–2858.

[10]Miles, J. W., "Nonlinear Surface Waves in Closed Basins," *Journal of Fluid Mechanics,* Vol. 75, No. 3, 1976, pp. 419–448.

[11]Lindenberg, K., and West, B. J., *The Nonequilibrium Statistical Mechanics of Open and Closed Systems,* VCH, New York, 1990.

[12]Yakubovich, V. A., and Starzhinskii, V. M., *Linear Differential Equations with Periodic Coefficients,* Wiley, New York, 1975, Vol. 1, Chap. II.

[13]Gardiner, C. W., *Handbook of Stochastic Methods,* Springer-Verlag, New York, 1985, Chap. 1.

[14]Landau, L. D., and Lifshitz, E. M., *Fluid Mechanics,* Pergamon, London, 1959, Chap. 2.